Supramolecular Aggregation of *m*-Nitrobenzoic Acid by C−H···O and O−H···O Hydrogen Bondings in the Crystalline Charge-Transfer Complexes with Aromatic Hydrocarbons

Takanori Suzuki* and Takashi Tsuji

Division of Chemistry, Graduate School of Science, Hokkaido University, Sapporo 060-0810, Japan

Takanori Fukushima, Setsuko Miyanari, and Tsutomu Miyashi

Department of Chemistry, Graduate School of Science, Tohoku University, Sendai 980-8578, Japan

Yasuyuki Sakata, Tsutomu Kouda, and Hiroki Kamiyama

Cosmo Research Institute, Satte, Saitama 340-0193, Japan

Received April 20, 1999

Charge-transfer complexation of *m*-nitrobenzoic acid (**1**) with aromatic hydrocarbons was found to exhibit size and shape selectivity: naphthalene or its 2,7-dimethyl and 2,3,6,7-tetramethyl derivatives failed to afford crystalline complexes with **1** whereas yellow crystals containing a stoichiometric amount of 2,3- or 2,6-dimethylnaphthalene, biphenylene, or anthracene were obtained by the direct method in CH_2Cl_2. X-ray analyses on these complexes have revealed dimer formation of **1** by O−H···O hydrogen bonding, yet the important structural motif observed as a common feature is the two-dimensional sheetlike network, in which the dimers of **1** are further connected by C−H···O hydrogen bonding to form a series of inclusion lattices that incorporate hydrocarbon guests. Such a supramolecular aggregation by C−H···O bonding was proven to take a significant part in the recognition properties of **1** to differentiate the dimethylnaphthalene isomers in its complexation process.

Recently much attention has been focused on noncovalent attractive interactions from the standpoint of supramolecular chemistry.[1] Molecular crystals are often regarded as the ultimate form of supramolecular assembly, and even a very weak force plays a significant role in determining the molecular packing in organic solids. Hydrogen bonding through short C−H···O contacts,[2,3] for example, has been proven one of the powerful tools to obtain supramolecular synthons.[5] Although a variety of structures formed by C−H···O bonding have been reported, only a few of them are discussed in terms of the functional properties of the resulting structures (e.g., NLO activity[6] or selective complexation with guests[7]). During the course of our study on the selective charge-transfer (CT) complexation of 2,4,7-trinitrofluorenone (TNF) with aromatic hydrocarbons (AHCs), we found that TNF molecules in these crystalline complexes are connected by C−H···O bonding to form "tape"-like networks, between which the AHC molecules are incorporated.[8] By considering the fact that the oxygens of NO_2 and the aromatic protons at ortho positions of NO_2 are the good acceptors and donors in C−H···O bonding, respectively, we assume that the many examples[9] of selective complexation of aromatic nitro compounds may be related with the inclusion lattice formation by C−H···O contacts in the crystal. We report here the selective complexation of *m*-nitrobenzoic acid (mNBA, **1**) with several AHCs and the unique crystal structures of the crystalline complexes determined by X-ray studies. It is worth noting that **1** can form a series of inclusion lattices such as a large hexagon structure[10] by the cooperative action of C−H···O and O−H···O hydrogen bondings, which leads to the recognition properties of **1** in its complexation process.

Results and Discussion

Complexation of mNBA 1 with AHC. Addition of AHC shown in Figure 1 to a colorless CH_2Cl_2 solution of **1** ($E^{red} = -1.23$ V vs SCE in MeCN) developed yellow color due to the weak CT interaction in solution (Scheme

(1) Lehn, J. M. *Supramolecular Chemistry*; VCH: Weinheim, 1995.
(2) Taylor, R., Kennard, O. *J. Am. Chem. Soc.* **1982**, *104*, 5063.
(3) Typical values for the H···O and C···O distances are 2.4−3.0 and 3.3−3.8 Å, respectively, in C−H···O hydrogen bonding. The geometrical definition for C−H···X hydrogen bondings has been discussed in recent papers (ref 4).
(4) Cotton, F. A.; Daniels, L. M.; Jordan, G. R., IV; Murillo, C. A. *Chem. Commun.* **1997**, 1673. Mascal, M. *Chem. Commun.* **1998**, 303. Steiner, T.; Desiraju, G. R. *Chem. Commun.* **1998**, 891.
(5) Desiraju, G. R. *Acc. Chem. Res.* **1996**, *29*, 441. Steiner, T. *Chem. Commun.* **1997**, 727.
(6) The noncentrosymmetric arrangements of molecules by O−H···O bonding were successfully obtained: Etter, M. C.; Grankenbach, G. M. *Chem. Mater.* **1989**, *1*, 10. Harris, K. D. M.; Hollingsworth, M. D. *Nature* **1989**, *341*, 19. NLO properties induced by C−H···O bonding in the crystal were reported very recently: Kawamata, J.; Inoue, K.; Inabe, T. *Bull. Chem. Soc. Jpn.* **1998**, *71*, 2777.
(7) Complementary binding through multiple C−H···O contacts in the crystal was proven effective for molecular recognition: Biradha, K.; Sharma, C. V. K.; Panneerselvam, K.; Shimoni, L.; Carrell, H. L.; Zacharias, D. E.; Desiraju, G. R. *Chem. Commun.* **1993**, 1473.
(8) Suzuki, T.; Fujii, H.; Miyashi, T.; Yamashita, Y. *J. Org. Chem.* **1992**, *57*, 6744.
(9) Foster, R. *Organic Charge-Transfer Complex*; Academic Press: London and New York, 1967.
(10) In the crystals of 4-substituted-3,5-dinitrobenzoic acid derivatives, large hexagon structures formed by C−H···O and O−H···O bondings were recently found which are similar to the case of 1,3,5-benzenetricarboxylic acid (ref 11): Pedireddi, V. R.; Jones, W.; Chorlton, A. P.; Docherty, R. *Chem. Commun.* **1996**, 987; *Tetrahedron Lett.* **1998**, *39*, 5409.

10.1021/jo990658z CCC: $18.00
Published on Web 08/25/1999

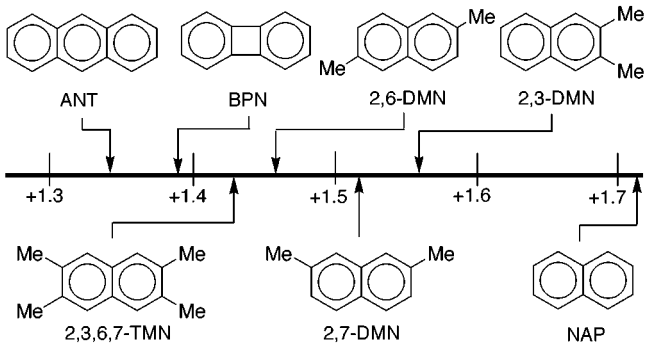

Figure 1. Oxidation potentials (E^{ox}/V vs SCE in MeCN) of AHC studied in this work. The upper four afforded crystalline CT complexes with **1** whereas the other three shown below the ruler did not.

Scheme 1

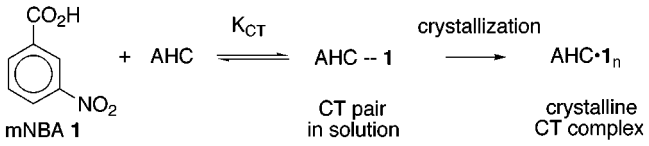

1). Slow evaporation of the solvent afforded the yellow crystalline complexes of **1** with 2,3-DMN (E^{ox} = +1.56 V), 2,6-DMN (+1.46 V), BPN (+1.39 V), and ANT (+1.34 V). The molar ratios of AHC to **1** are 1:2 except for the BPN complex (1:4), which were determined on the basis of combustion analyses. In the case of NAP (E^{ox} = +1.72 V), 2,7-DMN (+1.52 V), and 2,3,6,7-TMN[12] (+1.43 V), no crystalline complexes were obtained under similar conditions. Comparisons of E^{ox} indicate that the complexation of **1** does not depend on the electron-donating property of AHC, suggesting that the crystallization process is not usual CT complexation but rather that of host−guest type. It is worth noting that **1** can discriminate 2,6-DMN from the 2,7-isomer in light of the fact that they form a eutectic mixture upon crystallization.

Molecular Recognition of Dimethylnaphthalene (DMN) Isomers by mNBA 1, and X-ray Analysis of the 2,6-DMN·$\mathbf{1}_2$ Complex. Treatment of **1** with a mixture of 2,6- (55 mol %) and 2,7-DMN (55 mol %) in toluene resulted in the predominant complexation with 2,6-DMN (99.5 wt %), thus confirming the reported high selectivity for 2,6-DMN·$\mathbf{1}_2$ formation upon complexation of **1** with a C_{12} AHC mixture.[13] The association constants (K_{CT}) for the CT pairs (DMN···**1**) in solution were determined spectrophotometrically and found identical for 2,6- and 2,7-DMN (2.38 and 2.34 mol^{-1} dm^3, respectively), so that the differentiation by **1** is entirely absent in solution.

To clarify the origin of the selectivity for the solid-state complexation, the crystal structure of the 2,6-DMN·$\mathbf{1}_2$ complex was analyzed by X-ray studies, which have revealed the formation of a unique cyclic hexamer structure formed by **1** (Figure 2). The hexagon is large enough to leave a void that incorporates a 2,6-DMN molecule, connected to each other to form a coplanar sheetlike network in a "chicken-wire" motif. The shape of the cavity is not isotropic but elongated along one direction, thus suitable for the encapsulation of 2,6-DMN with the rough van der Waals (vdW) dimension of 12 × 7.5 Å.

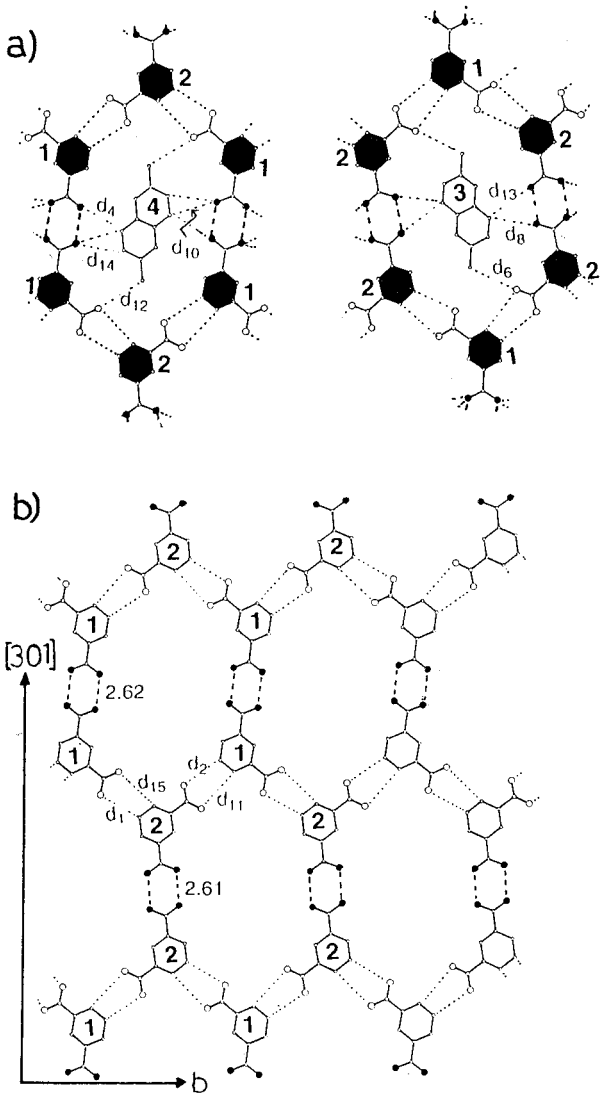

Figure 2. Packing arrangement in the 2,6-DMN·$\mathbf{1}_2$ complex. Oxygen atoms of $-CO_2H$ are shown by large filled circles whereas large open circles indicate those of $-NO_2$. There are two crystallographically independent molecules of **1** (molecules 1 and 2) and 2,6-DMN (molecules 3 and 4) in the crystal. The latter two are located on the inversion centers. (a) Two independent cyclic-hexamer structures. (b) Hexagons connected into a nearly coplanar chiken-wire network (2,6-DMN molecules are omitted for clarity). O−H···O hydrogen bondings (2.61 and 2.62 Å for O···O) are shown by broken lines. Short C···O contacts in C−H···O bondings (d_1, d_2, d_4, d_6, d_8, d_{10}, d_{11}, d_{12}, d_{13}, d_{14}, d_{15}) are indicated by dotted lines, and the distances and angles are given in Table 1. The deviations of the molecular plane from the neighbors are 0.03−1.80 Å (dihedral angle 0−7.0°) within the two-dimensional sheetlike network.

Hydrogen bondings through C−H···O (Table 1) and O−H···O contacts are operating simultaneously to form the hexagon, yet the latter only connect two molecules of **1** into a centrosymmetric dimer (*anti*-configuration in terms of the NO_2 group) as in the typical dimerization of carboxylic acids. It is the C−H···O bonding that connects the dimers into the infinite network, suggesting the

(11) Duchamp, D. J.; Marsh, R. E. *Acta Crystallogr.* **1969**, *B25*, 5. Herbstein, F. H.; Kapon, M.; Reisner, G. M. *Acta Crystallogr.* **1985**, *B41*, 348. Yaghi, O. M.; Li, H.; Groy, T. L. *J. Am. Chem. Soc.* **1996**, *118*, 9096.

(12) Rieke, R. D.; White, K.; McBride, E. *J. Org. Chem.* **1973**, *38*, 1430.

(13) Nagahama, S.; Shimada, K.; Kurozumi, S. Japan PAT. S47-38440, 1972.

Table 1. Interatomic Distances (d) and Angles (θ) for C−H···O Bonding in 2,6-DMN·1_2[a]

contact[b]	d(H···O)	d(C···O)	θ(C−H···O)	direction[c]
d_1: C(25)−H(25)···O(14)	2.51	3.41	142.4	lateral
d_2: C(15)−H(15)···O(24)	2.56	3.38	135.0	lateral
d_3: C(15)−H(15)···O(21)	2.60	3.37	129.5	stack
d_4: C(44)−H(44)···O(11)	2.63	3.56	143.7	lateral
d_5: C(46)−H(463)···O(13)	2.77	3.67	139.6	stack
d_6: C(36)−H(361)···O(23)	2.83	3.73	149.7	lateral
d_7: C(16)−H(16)···O(22)	2.83	3.65	132.1	stack
d_8: C(34)−H(34)···O(22)	2.86	3.51	119.8	lateral
d_9: C(36)−H(363)···O(12)	2.87	3.68	131.3	overlap
d_{10}: C(44)−H(44)···O(12)	2.89	3.55	119.3	lateral
d_{11}: C(14)−H(14)···O(23)	2.90	3.68	133.3	lateral
d_{12}: C(46)−H(461)···O(13)	2.91	3.84	153.7	lateral
d_{13}: C(34)−H(34)···O(21)	2.95	3.79	137.0	lateral
d_{14}: C(43)−H(43)···O(12)	2.95	3.59	119.1	lateral
d_{15}: C(24)−H(24)···O(13)	2.97	3.69	126.3	lateral

[a] Distances in angstroms and angles in degrees. The contacts with d(H···O) < 3.0, d(C···O) < 4.0, and θ(C−H···O) > 110° were accepted as C−H···O bonding. [b] Each C−H···O contact was assigned by d number to indicate the connected molecules in the crystal in Figure 2. The atom numbering of non-hydrogen atoms is shown in Figure 3. [c] Contacts within the sheet and those between sheets are indicated by lateral and stack, respectively.

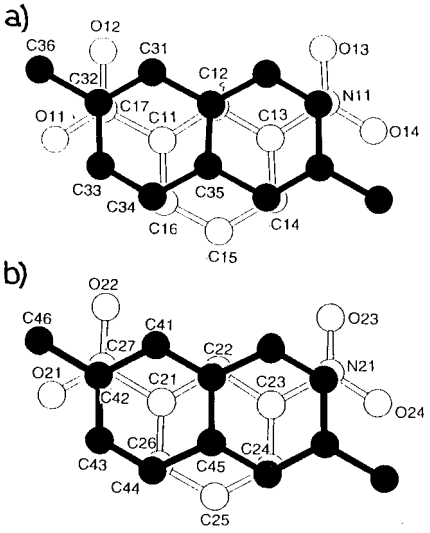

Figure 3. Two types of face-to-face overlaps of 2,6-DMN and **1** with the atom numbering scheme. Interplanar distances and dihedral angles are 3.50 Å and 3.3° in (a) and 3.44 Å and 1.1° in (b). There are two kinds of face-to-face overlaps between molecules of **1** (interplanar distances 3.44 and 3.51 Å; dihedral angles 0 and 0°) in the crystal, which are not shown in the figure.

important contribution of the weaker C−H···O bonding for the supramolecular aggregation in the crystal.[14] Short C−H···O contacts are also observed between the 2,6-DMN in the cavity and the hexagonal framework, thus preventing the guest from disordering its position in the cavity. Face-to-face columnar stacks of 2,6-DMN and **1** are formed perpendicularly to this coplanar arrangement (Figure 3), although the CT interaction through these overlaps seems marginal (vide infra).

Concomitant Inclusion of 2,7-DMN during the Complexation of mNBA 1 with 2,6-DMN. In contrast to the 2,6-DMN·$\mathbf{1}_2$ crystal, such a hexameric assembly does not exist in the uncomplexed crystals of **1**.[15]

(14) In some cases the weaker C−H···O bonding is more decisive than O−H···O bonding in determining the stable crystal packing: Sharma, C. V. K. M.; Desiraju, G. R. *Chem. Commun.* **1991**, 1239.

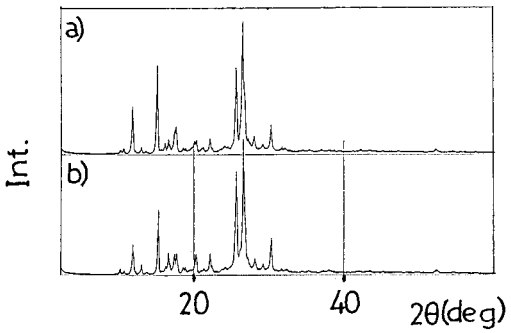

Figure 4. X-ray powder diffraction patterns (Cu Kα) of the (a) (2,6-DMN [74%] + 2,7-DMN [26%])·$\mathbf{1}_2$ complex and (b) pure 2,6-DMN·$\mathbf{1}_2$ complex. Note the close similarity in the two patterns.

Furthermore, there is no indication of supramolecular assembly of **1** in solution. Thus, the aggregation of **1** into the present hexagon results from the complexation with 2,6-DMN. By considering the close similarity in size and shape between 2,6- and 2,7-DMN, it is quite interesting that the 2,7-isomer induces neither the similar aggregation of **1** nor even crystalline complex formation. This phenomenon seems related to the different molecular symmetry of 2,6- (C_{2h}) and 2,7-DMN (C_{2v}).[16]

Another interesting feature is that the 2,7-isomer can be included in the cavity of the 2,6-DMN·$\mathbf{1}_2$ crystal under certain conditions. When a competitive complexation of **1** with a mixture of 2,6- and 2,7-DMN was conducted by using excess **1** (**1**:2,6-DMN:2,7-DMN = 100:33:33 mol %), the DMN·$\mathbf{1}_2$ complex thus obtained contained 15 wt % of the 2,7-isomer. By increasing the proportion of the 2,7-isomer in the DMN mixture, as much as 26 wt % of 2,7-DMN was incorporated into the complex. As shown in Figure 4, the resultant solid, (2,6-DMN [74%] + 2,7-DMN [26%])·$\mathbf{1}_2$, showed a powder X-ray diffraction pattern quite similar to that of the pure 2,6-DMN·$\mathbf{1}_2$, so that the 2,7-isomer must be accommodated in the cavity without disturbing the chicken-wire network of 2,6-DMN·$\mathbf{1}_2$.[17] These results clearly show that the high 2,6-/2,7-DMN selectivity can be achieved by aggregation of **1** into the porous supramolecular network, which is induced only in the case of 2,6-DMN with a suitable shape for the cavity. Lowering of the selectivity under certain conditions can be accounted for by the concomitant incorpora-

(15) Two modifications of **1** were analyzed by X-ray studies: (Stable form (*anti*-configuration of the dimer)) Dhaneshwar, N. N.; Tavale, S. S.; Pant, L. M. *Acta Crystallogr.* **1974**, *B30*, 583. (Unstable form (*syn*-configuration of the dimer)) Dhaneshwar, N. N.; Kulkarni, A. G.; Tavale, S. S.; Pant, L. M. *Acta Crystallogr.* **1975**, *B31*, 1978. Crystal structures were not given in these reports, so absence of the hexameric assembly in these crystals was confirmed by analyzing the packing arrangements on the basis of the reported atomic coordinates.

(16) Despite the low molecular symmetry of **1**, its dimer has pseudo-C_{2h} symmetry in the 2,6-DMN·$\mathbf{1}_2$ crystal (real symmetry is C_i for both the dimer and 2,6-DMN). It is probable that the 2,7-isomer (C_{2v}) having no centrosymmetric element induces the aggregation of **1** in a pseudo-C_{2v} manner to form the *syn*-dimer, which cannot be packed appropriately to give the chicken-wire structure. Successful transformation of molecular symmetry into supramolecular symmetry occurs in the crystal of layer-type structure in which the interlayer interaction is negligible: Thalladi, V. R.; Panneerselvam, K.; Carell, C. J.; Carrell, H. L.; Desiraju, G. R. *Chem. Commun.* **1995**, 341.

(17) According to the molecular dynamics by using the POLYGRAF program (Molecular Simulations), substitution of the 2,7-isomer for 2,6-DMN causes the vdW instability of 5.94 kcal mol^{-1} per site. This calculation was conducted by reproducing the network of **1** on the basis of the crystallographic data, and then the vdW energy was calculated after the position and orientation of the guest in the cavity were optimized.

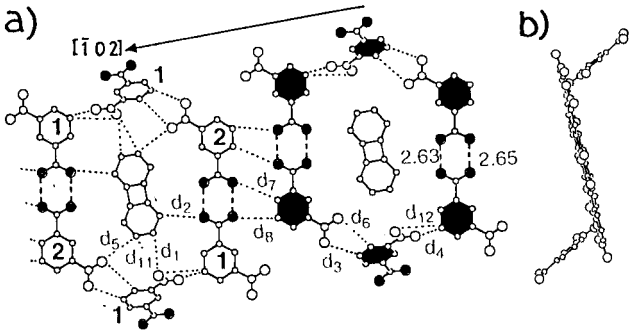

Figure 5. Packing arrangement in the BPN·**1**$_4$ complex: (a) top view, (b) side view. Oxygen atoms of $-CO_2H$ are shown by large filled circles whereas large open circles indicate those of $-NO_2$. There are two crystallographically independent molecules of **1** (molecules 1 and 2) in the crystal. The BPN molecules are located on the inversion centers. O−H···O hydrogen bondings (2.63 and 2.65 Å for O···O) are shown by broken lines. Short C···O contacts in C−H···O bondings (d_1, d_2, d_3, d_4, d_5, d_6, d_7, d_8, d_{11}, d_{12}) are indicated by dotted lines, and the distances and angles are given in Table 2. The deviations of the molecular plane from the neighbors are 0.25−1.25 Å (dihedral angle 0−5.9°) within the narrow strip of the corrugated sheet.

Table 2. Interatomic Distances (d) and Angles (θ) for C−H···O Bonding in BPN·1$_4$[a]

contact[b]	d(H···O)	d(C···O)	θ(C−H···O)	direction[c]
d_1: C(35)−H(35)···O(14)	2.56	3.31	134.8	lateral
d_2: C(36)−H(36)···O(11)	2.67	3.54	152.2	lateral
d_3: C(15)−H(15)···O(24)	2.72	3.52	140.7	lateral
d_4: C(15)−H(15)···O(13)	2.75	3.28	115.7	lateral
d_5: C(34)−H(34)···O(23)	2.82	3.48	126.3	lateral
d_6: C(14)−H(14)···O(23)	2.85	3.49	124.4	lateral
d_7: C(26)−H(26)···O(21)	2.93	3.85	161.3	lateral
d_8: C(25)−H(25)···O(12)	2.93	3.65	133.0	lateral
d_9: C(24)−H(24)···O(23)	2.94	3.43	113.0	stack
d_{10}: C(26)−H(26)···O(22)	2.95	3.46	114.7	stack
d_{11}: C(34)−H(34)···O(14)	2.96	3.51	117.0	lateral
d_{12}: C(15)−H(15)···O(14)	2.98	3.77	140.3	lateral

[a] Distances in angstroms and angles in degrees. The contacts with d(H···O) < 3.0, d(C···O) < 4.0, and θ(C−H···O) > 110° were accepted as C−H···O bonding. [b] Each C−H···O contact was assigned by d number to indicate the connected molecules in the crystal in Figure 5. The atom numbering of non-hydrogen atoms is shown in Figure 8. [c] Contacts within the sheet and those between sheets are indicated by lateral and stack, respectively.

tion of the 2,7-isomer in the cavity, suggesting that the cavity itself does not differentiate the detailed shape of the guests upon complexation.

Crystal Structures of BPN·1$_4$, 2,3-DMN·1$_2$, and ANT·1$_2$ Complexes. To explore the generality of the inclusion lattice formation by C−H···O bonding of **1**, X-ray structural analyses on the other three complexes of **1** were carried out. Their packing arrangements are shown in Figures 5−7, and Figures 8−10 show the overlapping patterns of **1** and AHCs, respectively.

It is evident from Figure 5 that the unique cyclic hexamer of **1** is also present in the crystal of the BPN·**1**$_4$ complex. As in the case of 2,6-DMN·**1**$_2$, the *anti*-dimers of **1** formed by O−H···O bonding are further connected into such a supramolecular assembly by C−H···O bonding (Table 2), and the BPN guest is incorporated at the center of the cavity exhibiting several short C−H···O contacts with the hexagon. The notable difference is the way in which the hexagons are annelated to each other; thus, the periphery of the hexagon is doubled in BPN·**1**$_4$ (Figure 5a). The corrugation of the whole two-dimensional network is, however, the largest difference of this structure from 2,6-DMN·**1**$_2$. Two molecules of **1** at the diagonal positions of the hexagon make a dihedral angle of 64° with the rest of the framework and the BPN guest in the cavity (Figure 5b). Such a deformation of the network from planarity may be related to the shorter dimension of BPN along the long axis (10.5 × 7.5 Å) than 2,6-DMN because folding at the two apexes of the hexagon affords better fitting of the cavity to the shape of BPN.

Table 3. Interatomic Distances (d) and Angles (θ) for C−H···O Bonding in 2,3-DMN·1$_2$[a]

contact[b]	d(H···O)	d(C···O)	θ(C−H···O)	direction[c]
d_1: C(37)−H(37)···O(23)	2.33	3.34	155.0	lateral
d_2: C(25)−H(25)···O(13)	2.41	3.44	158.4	lateral
d_3: C(14)−H(14)···O(14)	2.42	3.48	167.8	lateral
d_4: C(35)−H(35)···O(24)	2.65	3.49	134.9	lateral
d_5: C(36)−H(36)···O(23)	2.66	3.61	146.3	lateral
d_6: C(15)−H(15)···O(21)	2.70	3.54	134.2	lateral
d_7: C(41)−H(411)···O(14)	2.76	3.69	142.6	stack
d_8: C(16)−H(16)···O(11)	2.78	3.79	155.9	lateral
d_9: C(38)−H(38)···O(22)	2.79	3.79	154.8	lateral
d_{10}: C(42)−H(421)···O(14)	2.80	3.45	118.0	overlap
d_{11}: C(26)−H(26)···O(24)	2.97	3.59	116.5	stack

[a] Distances in angstroms and angles in degrees. The contacts with d(H···O) < 3.0, d(C···O) < 4.0, and θ(C−H···O) > 110° were accepted as C−H···O bonding. [b] Each C−H···O contact was assigned by d number to indicate the connected molecules in the crystal in Figure 6. The atom numbering of non-hydrogen atoms is shown in Figure 9. [c] Contacts within the sheet and those between sheets are indicated by lateral and stack, respectively.

The size (10.5 × 7.5 Å) similar to that of BPN but different molecular symmetry may result in another kind of inclusion lattice by C−H···O bonding (Table 3) in the 2,3-DMN·**1**$_2$ crystal (Figure 6). A noteworthy feature is the *syn*-configuration of the O−H···O dimer of **1**, which is absent in the other three X-ray structures where the AHC guest is centrosymmetric. Such dimers are connected along the [011] axis by C−H···O bonding to form the coplanar "tape" networks, between which is incorporated an array of 2,3-DMN. It looks as if the lower three molecules of **1** out of the shaded six in Figure 6a were slid along the [011] direction to miss the cyclization into the hexagon because the geometrical features of 2,3-DMN are not suitable for the cavity of the cyclic hexamer.

The similar inclusion lattice of the tape motif is also observed in the ANT·**1**$_2$ crystal (Figure 7). The O−H···O *anti*-dimers related by translation along the *a* axis are connected by C−H···O bonding (Table 4), and the ANT guest is located on the crystallographic center of symmetry, thus making up the very simple packing arrangement. Several C−H···O contacts including the shortest one are observed between ANT and **1**, which may take a part in allocating the ANT molecules within the same plane of the tape networks of **1**, leading to the coplanar two-dimensional arrangement as a whole (Figure 7b).

No complexation of **1** with 2,3,6,7-TMN, which has molecular dimensions similar to those of ANT (11.5 × 7.5 Å), might be accounted for by the fact that C(sp^3)−H is less acidic than C(sp^2)−H, thus affording only weaker C−H···O bonds[18] between the Me protons and O atoms of **1** in the hypothetical crystal structure of the 2,3,6,7-TMN complex. Deviation of C−H bonds of Me groups from the aromatic plane also seems unfavorable for Me

(18) Correlation between the C−H acidity and the strength of the C−H···O bond has been established: Pedireddi, V. R.; Desiraju, G. R. *Chem. Commun.* **1992**, 998.

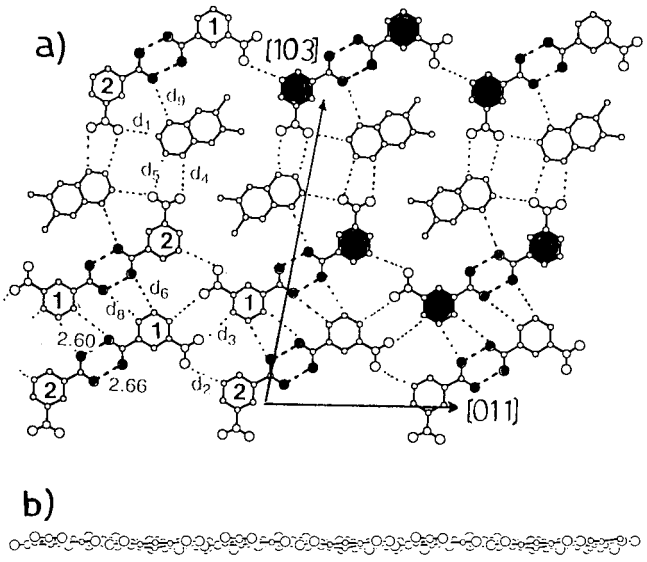

Figure 6. Packing arrangement in the 2,3-DMN·$\mathbf{1}_2$ complex: (a) top view, (b) side view. Oxygen atoms of $-CO_2H$ are shown by large filled circles whereas large open circles indicate those of $-NO_2$. There are two crystallographically independent molecules of **1** (molecules 1 and 2) in the crystal. O−H···O hydrogen bondings (2.60 and 2.66 Å for O···O) are shown by broken lines. Short C···O contacts in C−H···O bondings (d_1, d_2, d_3, d_4, d_5, d_6, d_8, d_9) are indicated by dotted lines, and the distances and angles are given in Table 3. The deviations of the molecular plane from the neighbors are 0.03−0.99 Å (dihedral angle 0−3.9°) within the two-dimensional sheetlike network.

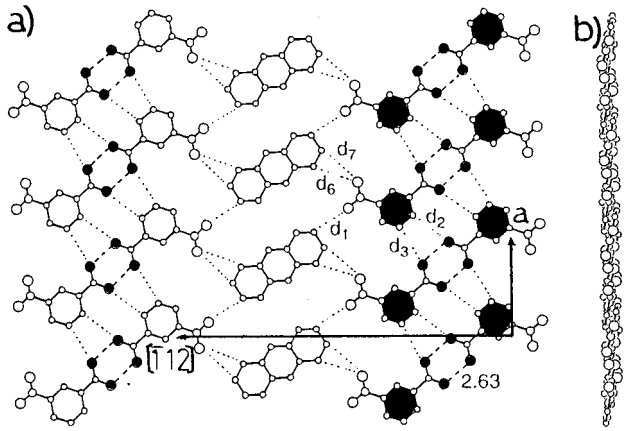

Figure 7. Packing arrangement in the ANT·$\mathbf{1}_2$ complex: (a) top view, (b) side view. Oxygen atoms of $-CO_2H$ are shown by large filled circles whereas large open circles indicate those of $-NO_2$. The ANT molecules are located on the inversion centers. O−H···O hydrogen bondings (2.63 Å for O···O) are shown by broken lines. Short C···O contacts in C−H···O bondings (d_1, d_2, d_3, d_6, d_7) are indicated by dotted lines, and the distances and angles are given in Table 4. The deviations of the molecular plane from the neighbors are 0.31−1.83 Å (dihedral angle 0−4.3°) within the two-dimensional sheetlike network.

protons to participate in C−H···O bonding by considering the directional preference[2] of this weak force as well as the coplanarity of the resulting networks.[19] In fact, only two C−H···O contacts involving Me protons are observed in 2,6-DMN·$\mathbf{1}_2$ (d_6 and d_{12} in Table 1 and Figure 2a), and no Me protons of 2,3-DMN are involved in its complex (Figure 6a). It is suggested that the AHC with many Me groups around its periphery would not be a good guest

Table 4. Interatomic Distances (d) and Angles (θ) for C−H···O Bonding in ANT·$\mathbf{1}_2$[a]

contact[b]	d(H···O)	d(C···O)	θ(C−H···O)	direction[c]
d_1: C(12)−H(12)···O(4)	2.56	3.27	130.5	lateral
d_2: C(6)−H(6)···O(1)	2.59	3.44	146.6	lateral
d_3: C(5)−H(5)···O(2)	2.65	3.43	138.4	lateral
d_4: C(12)−H(12)···O(3)	2.71	3.51	140.7	stack
d_5: C(11)−H(11)···O(2)	2.87	3.66	132.4	stack
d_6: C(14)−H(14)···O(3)	2.89	3.55	127.1	lateral
d_7: C(13)−H(13)···O(3)	2.98	3.59	122.7	lateral

[a] Distances in angstroms and angles in degrees. The contacts with d(H···O) < 3.0, d(C···O) < 4.0, and θ(C−H···O) > 110° were accepted as C−H···O bonding. [b] Each C−H···O contact was assigned by d number to indicate the connected molecules in the crystal in Figure 7. The atom numbering of non-hydrogen atoms is shown in Figure 10. [c] Contacts within the sheet and those between sheets are indicated by lateral and stack, respectively.

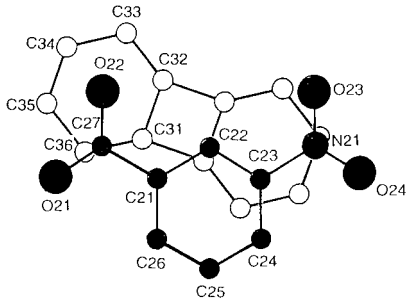

Figure 8. Face-to-face overlaps of BPN and **1** with the atom numbering scheme. The interplanar distance and dihedral angle are 3.39 Å and 3.8°. There is a face-to-face overlap between molecules of **1** (interplanar distance 3.37 Å; dihedral angle 2.2°) in the crystal, which are not shown in the figure.

for the complexation with aromatic nitro compounds in terms of the thermodynamic stabilization by C−H···O bonding in the crystal despite the donating properties of Me groups to enhance the CT interaction.

Another factor affecting the complexation and/or the packing motif of the resultant crystals may be $\pi-\pi$ interaction through the face-to-face overlap of molecules. On the basis of the MO coefficients in the LUMO of **1** and HOMOs of AHCs, some overlaps shown in Figures 3 and 8−10 seem favorable for the orbital interaction between them. The interplanar distances of 3.39−3.55 Å, however, are similar to or beyond the sum of vdW radii (3.40 Å). So, CT interaction may stabilize the crystalline state of all the complexes but would not be the governing factor in determining the crystal packing in these complexes.

Conclusion

Presently we are not at the level at which we can predict the shape and properties of the inclusion lattice formed by **1** for a given AHC. This is partly because of the high sensitivity of the packing arrangement to the size and shape of the components as exemplified by the quite different behavior of **1** with NAP, BPN, and ANT having the same molecular symmetry and similar dimen-

(19) The "sheet"-like networks in the three complexes out of four exhibit fairly good coplanarity as a common feature. It is also noteworthy that each strip of the corrugated sheet network in BPN·$\mathbf{1}_4$ shows the coplanar arrangement. Previously it was shown that C−H···O bonding is effective in steering flat molecules into the adoption of layered crystal structures: Sarma, J. A. R. P.; Desiraju, G. R. *Acc. Chem. Res.* **1986**, *19*, 222; *J. Chem. Soc., Perkin Trans. 2* **1987**, 1195.

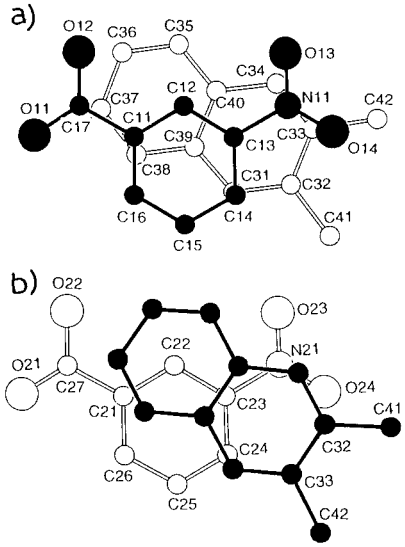

Figure 9. Two kinds of face-to-face overlaps of 2,3-DMN and **1** with the atom numbering scheme. Interplanar distances and dihedral angles are 3.48 Å and 3.9° in (a) and 3.52 Å and 3.3° in (b). There is a face-to-face overlap between molecules of **1** (interplanar distance 3.47 Å; dihedral angle 2.2°) in the crystal, which are not shown in the figure.

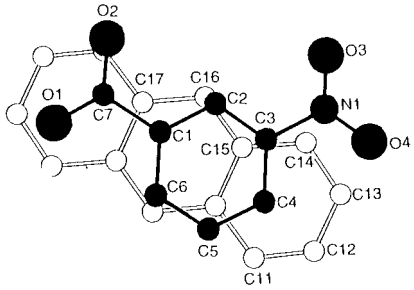

Figure 10. Face-to-face overlaps of ANT and **1** with the atom numbering scheme. The interplanar distance and dihedral angle are 3.55 Å and 4.3°. There is a face-to-face overlap between molecules of **1** (interplanar distance 3.31 Å; dihedral angle 0°) in the crystal, which are not shown in the figure.

sions ((9−11.5) × 7.5 Å). Yet, all the results clearly show that C−H···O bonding is taking a part not only in the determination of crystal packing but also in the supramolecular aggregation to induce the functional properties (e.g., molecular recognition) of the resulting structures. At the same time, the present work has added experimental support to the hypothesis that the recognition properties of aromatic nitro compounds against AHCs would come from the inclusion lattice formation by C−H···O bonding although large accumulation of the case studies such as this is still necessary before making general concluding remarks.

Experimental Section

Complexation of mNBA (1) with 2,6-DMN. To a colorless solution of **1** (66 mg, 0.40 mmol) in CH_2Cl_2 (4 mL) was added 2,6-DMN (250 mg, 1.60 mmol) at room temperature. The resultant yellow solution was allowed to stand with slow evaporation of the solvent to 1.5 mL. Large yellow rods (67 mg) were filtered and washed with CH_2Cl_2 (0.5 mL × 2) to obtain the 1:2 complex (2,6-DMN·**1**$_2$) in 68% yield: mp 100−101 °C dec. Anal. Calcd for $C_{26}H_{22}N_2O_8$: C, 63.67; H, 4.52; N, 5.71. Found: C, 63.71; H, 4.60; N, 5.72. The IR spectrum of the complex resembles that of pure **1** because 2,6-DMN does not show strong absorptions and its molar proportion is only half that of **1**. The ^{1}H NMR spectrum in $CDCl_3$ is almost identical to the superimposition of two components (2,6-DMN and **1**) because the complex dissociates upon dissolution. Very slight upfield shifts of less than 0.01 ppm were noticed by careful comparisons of the spectra which are due to the CT pair formation in solution: 2,6-DMN (0.02 M in $CDCl_3$, 400 MHz) δ/ppm 2.489 (12H, s), 7.272 (2H, dd, 8.3, 1.0 Hz), 7.560 (2H, br s), 7.649 (2H, d, 8.3 Hz); **1** (0.04 M in $CDCl_3$, 400 MHz) δ/ppm 7.726 (1H, dd, 7.8, 7.8 Hz), 8.456 (1H, ddd, 7.8, 1.5, 1.0 Hz), 8.499 (1H, ddd, 7.8, 2.4, 1.0 Hz), 8.968 (1H, ddd, 2.4, 1.5 Hz); 2,6-DMN·**1**$_2$ (0.02 M in $CDCl_3$, 400 MHz) δ/ppm 2.489 (12H, s), 7.268 (2H, dd, 8.3, 1.0 Hz), 7.555 (2H, br s), 7.646 (2H, d, 8.3 Hz), 7.717 (2H, dd, 7.8, 7.8 Hz), 8.451 (2H, ddd, 7.8, 1.5, 1.0 Hz), 8.493 (2H, ddd, 7.8, 2.4, 1.0 Hz), 8.963 (2H, ddd, 2.4, 1.5 Hz). Competitive complexations of **1** with a mixture of 2,6- and 2,7-DMN were conducted under experimental conditions similar to those reported in the literature.[13]

Complexation of mNBA (1) with Other AHCs. Other complexes were obtained by the direct method similar to that in the case of 2,6-DMN·**1**$_2$. Their decomposition points and the analytical values are as follows. BPN (1:4) complex: yellow efflorescent plates; mp 128−131 °C dec. Anal. Calcd for $C_{40}H_{28}N_4O_{16}$: C, 58.54; H, 3.44; N, 6.83. Found: C, 58.45; H, 3.62; N, 6.80. 2,3-DMN (1:2) complex: pale yellow efflorescent plates; mp 100−101 °C dec. Anal. Calcd for $C_{26}H_{22}N_2O_8$: C, 63.67; H, 4.52; N, 5.71. Found: C, 63.71; H, 4.60; N, 5.72. ANT (1:2) complex: yellow cubes; mp 133−135 °C dec. Anal. Calcd for $C_{28}H_{20}N_2O_8$: C, 65.62; H, 3.93; N, 5.47. Found: C, 65.69; H, 3.93; N, 5.43.

Measurement of Redox Potentials. The reduction potential of **1** (E^{red}) and oxidation potentials (E^{ox}) of AHCs were measured by cyclic voltammetry in dry MeCN containing 0.1 mol dm^{-3} Et_4NClO_4 as a supporting electrolyte. All the values shown in the text are in E/V vs SCE, and Pt wire was used as the working electrode. In the case of irreversible waves, half-wave potentials were estimated from the anodic peak potentials (E^{pa}) as $E^{ox} = E^{pa} - 0.03$ V.

Determination of K_{CT}. Association constants for CT pairs (DMN···**1**) were determined photospectroscopically in the presence of a large excess of 2,6- or 2,7-DMN in $CHCl_3$ at 25 °C using the Benesi−Hildebrand equation.[20] In both cases linear correlations were observed, suggesting the 1:1 molar ratio for the CT pairs in solution. The concentration of **1** is (5.99−6.20) × 10^{-2} mol dm^{-3}, and those for DMN are (0.32−1.28) mol dm^{-3}.

X-ray Analyses on Crystalline Complexes of mNBA (1). Crystal Data for 2,6-DMN·1$_2$. $C_{26}H_{22}N_2O_8$, M = 490.46, pale yellow plates (toluene), 0.3 × 0.3 × 0.1 mm, triclinic $P\bar{1}$ bar, a = 10.772(5) Å, b = 12.013(4) Å, c = 10.507(4) Å, α = 105.97(3)°, β = 115.46(3)°, γ = 83.87(4)°, V = 1180.2(9) Å^3, ρ(Z=2) = 1.381 g cm^{-1}. A total of 4879 unique data ($2\theta_{max}$ = 52°) was measured at T = 296 K in the ω−2θ scan mode (Mo Kα radiation, λ = 0.710 69 Å). No absorption correction was applied (μ = 0.969 cm^{-1}). The structure was solved by the direct method (Rantan) and refined by a block-matrix least-squares method on F with anisotropic temperature factors for non-hydrogen atoms. Hydrogen atoms were located at the calculated positions and included in the refinement. The final R value is 0.0677 for 2991 reflections with $F > 3\sigma F$ and 406 parameters.

Crystal Data for BPN·1$_4$. $C_{40}H_{28}N_4O_{16}$, M = 820.66, efflorescent pale yellow plates (CH_2Cl_2), 0.35 × 0.3 × 0.2 mm (sealed in a glass capillary), monoclinic $P2_1/n$, a = 11.837(4) Å, b = 27.024(9) Å, c = 6.044(3) Å, β = 104.26(3)°, V = 1873.7(10) Å^3, ρ (Z=2) = 1.455 g cm^{-1}. A total of 3819 unique data ($2\theta_{max}$ = 53°) was measured at T = 298 K in the ω scan mode (Mo Kα radiation, λ = 0.710 69 Å). No absorption correction was applied (μ = 1.073 cm^{-1}). The structure was solved by the direct method (Crystan) and refined by a full-matrix least-squares method on F with anisotropic tempera-

(20) Benesi, H. A.; Hidebrand, J. H. *J. Am. Chem. Soc.* **1960**, *82*, 2134.

ture factors for non-hydrogen atoms. Hydrogen atoms of hydroxy groups were picked up from the *D*-map, and others were located at the calculated positions. Their isotropic temperature factors were included in the refinement. The final *R* value is 0.0565 for 2904 reflections with $I > 2\sigma I$ and 280 parameters.

Crystal Data for 2,3-DMN·$\mathbf{1}_2$. $C_{26}H_{22}N_2O_8$, $M = 490.46$, efflorescent yellow plates (CH_2Cl_2), 0.3 × 0.3 × 0.2 mm (sealed in a glass capillary), triclinic $P\bar{1}$ bar, $a = 10.919(2)$ Å, $b = 14.754(2)$ Å, $c = 7.890(1)$ Å, $\alpha = 103.47(1)°$, $\beta = 100.22(1)°$, $\gamma = 99.17(1)°$, $V = 1189.5(3)$ Å^3, $\rho(Z = 2) = 1.370$ g cm^{-1}. A total of 4673 unique data ($2\theta_{max} = 52°$) was measured at $T = 296$ K in the $\omega-2\theta$ scan mode (Mo Kα radiation, $\lambda = 0.710\ 69$ Å). No absorption correction was applied ($\mu = 0.96$ cm^{-1}). The structure was solved by the direct method (Texsan) and refined by a full-matrix least-squares method on *F* with anisotropic temperature factors for non-hydrogen atoms. Hydrogen atoms were located at the calculated positions. Their isotropic temperature factors were included in the refinement. The final *R* and *Rw* values are 0.0574 and 0.0622 for 2041 reflections with $I > 3\sigma I$ and 345 parameters.

Crystal Data for ANT·$\mathbf{1}_2$. $C_{28}H_{20}N_2O_8$, $M = 512.50$, yellow cubes (CH_2Cl_2), 0.5 × 0.5 × 0.5 mm, triclinic $P\bar{1}$ bar, $a = 7.271(2)$ Å, $b = 8.374(2)$ Å, $c = 11.112(3)$ Å, $\alpha = 69.24(2)°$, $\beta = 71.09(2)°$, $\gamma = 86.82(2)°$, $V = 597.1(3)$ Å^3, $\rho(Z=1) = 1.425$ g cm^{-1}. A total of 2590 unique data ($2\theta_{max} = 55°$) was measured at $T = 298$ K in the $\omega-2\theta$ scan mode (Mo Kα radiation, $\lambda = 0.710\ 69$ Å). No absorption correction was applied ($\mu = 0.991$ cm^{-1}). The structure was solved by the direct method (Crystan) and refined by a full-matrix least-squares method on *F* with anisotropic temperature factors for non-hydrogen atoms. The hydrogen atom of hydroxy group was picked up from the *D*-map, and others were located at the calculated positions. Their isotropic temperature factors were included in the refinement. The final *R* value is 0.0561 for 2261 reflections with $I > 2\sigma I$ and 181 parameters.

Acknowledgment. We thank Professor Tamotsu Inabe (Hokkaido University) for the use of the X-ray structure analysis system. Elemental analyses were carried out by Ms. Akiko Maeda, and NMR spectra were measured by Ms. Kazuyo Nakaoka at the Center for Instrumental Analysis (Hokkaido University). Financial support (to T.S.) by the Asahi Glass Foundation and by Izumi Science and Technology Foundation is gratefully acknowledged.

Supporting Information Available: Details of X-ray structural analyses of 2,6-DMN·$\mathbf{1}_2$, BPN·$\mathbf{1}_4$, 2,3-DMN·$\mathbf{1}_2$, and ANT·$\mathbf{1}_2$. This material is available free of charge via the Internet at http://pubs.acs.org.

JO990658Z